

Whistler instability stimulated by the suprathermal electrons present in space plasmas

M. Lazar^{1,2} • R. A. López¹ • S. M. Shaaban^{1,3} •
S. Poedts¹ • H. Fichtner²

Abstract In the absence of efficient collisions, deviations from thermal equilibrium of plasma particle distributions are controlled by the self-generated instabilities. The whistler instability is a notorious example, usually responsible for the regulation of electron temperature anisotropy $A = T_{\perp}/T_{\parallel} >$ (with \perp, \parallel respective to the magnetic field direction) observed in space plasmas, e.g., solar wind and planetary magnetospheres. Suprathermal electrons present in these environments change the plasma dispersion and stability properties, with expected consequences on the kinetic instabilities and the resulting fluctuations, which, in turn, scatter the electrons and reduce their anisotropy. In order to capture these mutual effects we use a quasilinear kinetic approach and PIC simulations, which provide a comprehensive characterization of the whistler instability under the influence of suprathermal electrons. Analysis is performed for a large variety of plasma conditions, ranging from low-beta plasmas encountered in outer corona or planetary magnetospheres to a high-beta solar wind characteristic to large heliospheric distances. Enhanced by the suprathermal electrons, whistler fluctuations stimulate the relaxation of temperature anisotropy, and this influence of suprathermals increases with plasma beta parameter.

M. Lazar
R. A. López
S. M. Shaaban
S. Poedts
H. Fichtner

¹Centre for Mathematical Plasma Astrophysics, Celestijnenlaan 200B, B-3001 Leuven, Belgium.

²Institut für Theoretische Physik, Lehrstuhl IV: Weltraum- und Astrophysik, Ruhr-Universität Bochum, D-44780 Bochum, Germany.

³Theoretical Physics Research Group, Physics Department, Faculty of Science, Mansoura University, 35516, Egypt.

Keywords plasmas - instabilities - solar wind

1 Introduction and motivation

Whistler instability is known as the instability of electromagnetic electron-cyclotron (EMEC) modes, driven unstable by the free energy of anisotropic electrons, in particular, those with anisotropic temperatures $T_{\perp} > T_{\parallel}$, (where \perp, \parallel denote directions respective to the local magnetic field lines) (Kennel and Petschek 1966). This instability has given rise to a particular interest in space plasmas, where it is often invoked to explain, for instance, the electromagnetic fluctuations detected at kinetic scales in the solar wind and terrestrial magnetosphere (Wilson III et al. 2009, 2013; Kellogg et al. 2011) and, implicitly, the role played by these fluctuations in the relaxation of temperature anisotropies (Štverák et al. 2008; Schriver et al. 2010; An et al. 2017; Kim et al. 2017). The interested readers may also consult Stenzel (1999) for a review of the early observations of whistlers in the solar wind and planetary magnetospheres.

The knowledge of the velocity distribution of electrons is particularly important for a realistic characterization of whistler instability and its implications. The in-situ measurements in space plasmas across the heliosphere reveal non-thermal distributions with non-Maxwellian suprathermal tails (Vasyliunas 1968; Maksimovic et al. 1997; Pierrard and Lazar 2010). In theory commonly adopted are the idealized (bi-)Maxwellian models (Gary 1993; Yoon 2017), which can reproduce only the low-energy core of the observed distributions. The high density of the core population (with more than 90% of total number of particles) is invoked as a justification, although an important amount of heat and kinetic energy is transported by the suprathermal populations (Pierrard and Lazar 2010; Lazar et al.

2015). Suprathermal electrons are ubiquitous in the solar wind enhancing the high-energy tails of the observed distributions and highly contrasting with the (bi-)Maxwellian core (Maksimovic et al. 1997). The role of these hotter electrons in the excitation of whistler instability has been anticipated in the original study of Kennel and Petschek (1966), though these authors have treated only waves resonant with electrons on the high-energy tail, where the number of resonant particles, and therefore the growth rate, is small. In the present paper we present a complete analysis of the whistler instability resulting from the interplay of both thermal and suprathermal electrons, and outline the effects of suprathermal electrons on the enhanced fluctuations and the relaxation of temperature anisotropy.

As an intimate component of the non-equilibrium plasmas, suprathermal populations are expected to be an important source of free energy, triggering various plasma processes (Hapgood et al. 2011). If we refer to kinetic instabilities driven by temperature anisotropies, many of the existing studies involving a bi-Kappa representation fail to describe the effects of suprathermal populations. Thus, contrary to expectations, suprathermals appear to have an inhibiting effect, and, particularly for the whistler instability, stimulation has been found only for marginal conditions, i.e., for very low anisotropies $1 \lesssim T_{\perp}/T_{\parallel} < 2$ (Mace and Sydora 2010; Lazar et al. 2013, 2018a). However, in our study we apply a straightforward comparative analysis recently proposed to outline suprathermal populations and their implications by contrasting the observed Kappa distribution with a quasi-thermal core population (Lazar et al. 2015, 2016). The anisotropic electrons are described by a single or global bi-Kappa (or bi-Lorentzian) distribution function (Summers and Thorne 1991), which is nearly bi-Maxwellian at low energies reproducing the core, and decreases as a power-law at higher energies (Pierrard and Lazar 2010; Lazar et al. 2015, 2017a). Dual models involving Kappa or bi-Kappa functions to reproduce only suprathermal (or halo) population in combination with a bi-Maxwellian to describe the core (Maksimovic et al. 2005; Štverák et al. 2008; Lazar et al. 2017a; Wilson III et al. 2019), may give better fits to the observations than a single bi-Kappa incorporating both the core and halo populations (Lazar et al. 2017a). However, a single, or global bi-Kappa representation is more often invoked in theoretical analyses due to a reduced number of parameters involved (Mace and Sydora 2010; Lazar et al. 2013, 2015), and has a particular relevance for describing the effects of suprathermal populations (Lazar et al. 2015, 2016). It may also be motivated observationally, by the solar wind electron data collected by spacecraft

missions from different heliospheric distances (Štverák et al. 2008), which are dominated by the core (subscript c) and halo (subscript h) populations with similar anisotropies, either both with $A_{c,h} > 1$ or both with $A_{c,h} < 1$ (Pierrard et al. 2016). These states with correlated anisotropies of the core and halo populations are the most unstable and most relevant for instabilities (of interest for us being those with $A_c \simeq A_h > 1$), and for the sake of simplicity and generality, we assume them well described by a single bi-Kappa, see also Appendix A. A general analysis of suprathermal populations and their effects becomes indeed straightforward, by contrasting with the results obtained for quasi-thermal core well approached by the bi-Maxwellian limit $\kappa \rightarrow \infty$, see Appendix A and Lazar et al. (2015, 2016, 2018b).

Such a direct comparison leads to a systematic stimulation of linear growth rates in the presence of suprathermal populations, and not only for the whistler instability (Lazar et al. 2015; Viñas et al. 2015; Shaaban et al. 2016, 2017; Lazar et al. 2017b; Shaaban et al. 2018, 2019a). In order to test these predictions from linear theory here we propose a comprehensive study of whistler instability employing quasilinear theory (section 2) and particle-in-cell (PIC) simulations (section 3). The effects of suprathermal electrons are evaluated for a wide range of values of the plasma beta parameter, covering heliospheric plasma conditions specific to the solar wind and planetary magnetospheres.

2 Quasilinear approach

We assume a sufficiently homogeneous and collisionless plasma of bi-Kappa distributed electrons (subscript e) and Maxwellian isotropic protons (subscript p), see Appendix A. Whistler modes are described by the linear (instantaneous) dispersion relation

$$\tilde{k}^2 = A - 1 + \frac{A \tilde{\omega} - A - 1}{\tilde{k} \sqrt{\beta_{e,\parallel}}} Z_{\kappa} \left(\frac{\tilde{\omega} - 1}{\tilde{k} \sqrt{\beta_{e,\parallel}}} \right) + \frac{\tilde{\omega}}{\tilde{k} \sqrt{\mu \beta_p}} Z_p \left(\frac{\mu \tilde{\omega} + 1}{\tilde{k} \sqrt{\mu \beta_p}} \right), \quad (1)$$

where $\tilde{\omega} = \omega/|\Omega_e|$ is the normalized wave frequency $\omega = \omega_r + i\gamma$, $\tilde{k} = kc/\omega_{p,e}$ is the normalized wave-number k , c is the speed of light in vacuum, $\omega_{p,e} = \sqrt{4\pi n_0 e^2/m_e}$ and $\Omega_e = eB_0/(mc)$ are, respectively, the plasma and cyclotron frequencies of electrons, $\mu = m_p/m_e = 1836$ is the proton-electron mass ratio. Plasma beta parameters $\beta_{\parallel,\perp} = 8\pi n_0 k_B T_{\parallel,\perp}/B_0^2$, temperature anisotropy, assumed $A = T_{\perp}/T_{\parallel} > 1$, and plasma dispersion functions Z_{κ} and Z are explained in detail in Appendices A and B.

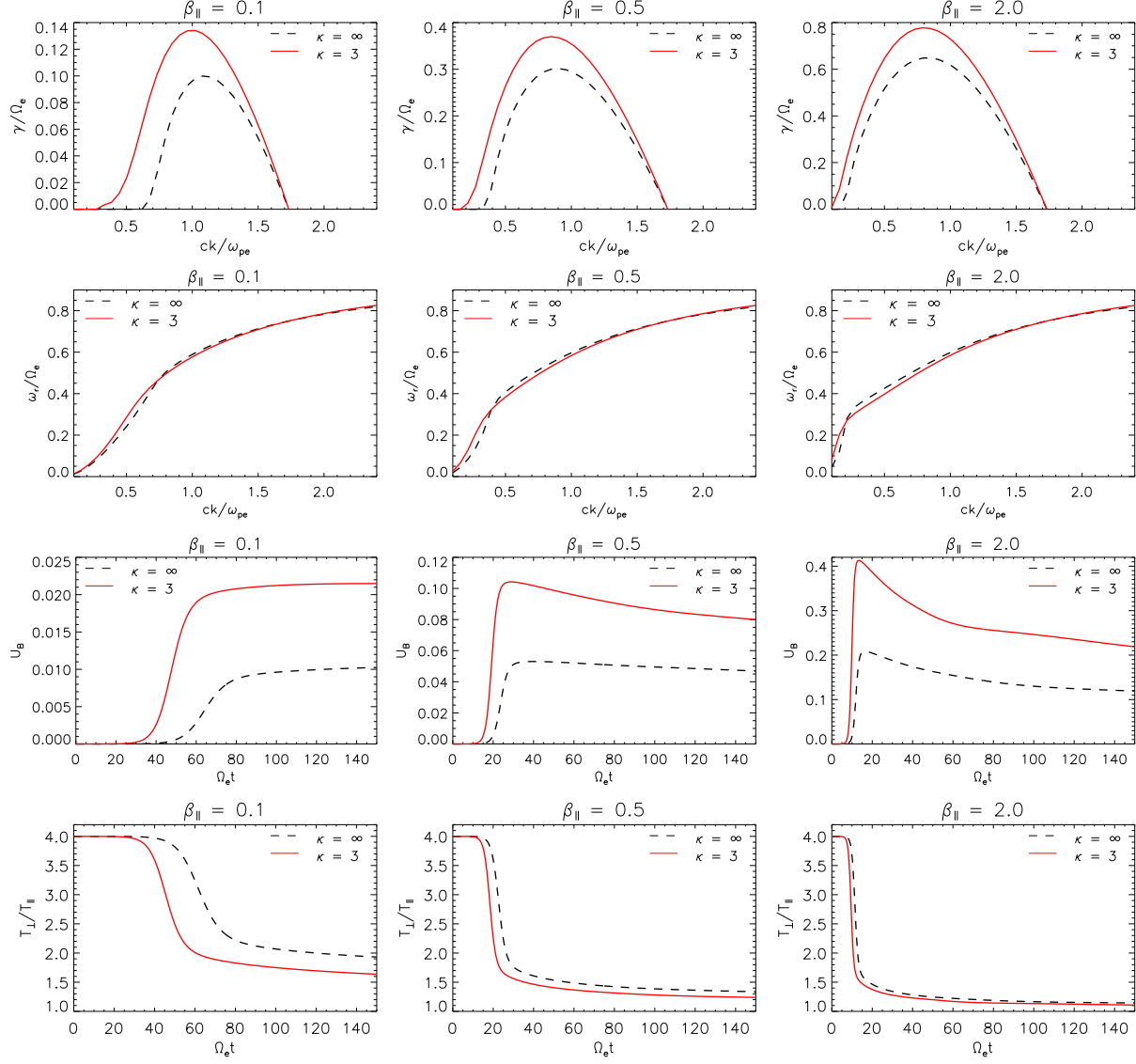


Fig. 1 Systematic stimulation of the whistler instability (growth rate γ , wave-frequency ω_r , magnetic power U_B) and subsequent relaxation of temperature anisotropy (T_{\perp}/T_{\parallel}) in the presence of suprathermals: three distinct cases corresponding to $\beta_{c,\parallel}(0) = \beta_{\parallel}(0) = 0.1, 0.5, 2.0$, see discussion in the text.

In the diffusion approximation time evolution of the electron distribution is described by the following quasi-linear (QL) equation (Yoon 2017; Lazar et al. 2018a)

$$\frac{\partial f_e}{\partial t} = \frac{ie^2}{4m_e^2 c^2} \int_{-\infty}^{\infty} \frac{dk}{k} \left[(\omega^* - kv_{\parallel}) \frac{\partial}{v_{\perp} \partial v_{\perp}} + k \frac{\partial}{\partial v_{\parallel}} \right] \times \frac{v_{\perp}^2 \delta B^2(k, \omega)}{\omega - kv_{\parallel} - |\Omega_e|} \left[(\omega - kv_{\parallel}) \frac{\partial}{v_{\perp} \partial v_{\perp}} + k \frac{\partial}{\partial v_{\parallel}} \right] f_e \quad (2)$$

combined with the wave kinetic equation

$$\frac{\partial \delta B^2(k)}{\partial t} = 2\gamma_k \delta B^2(k). \quad (3)$$

Here $\delta B^2(k)$ is the wave energy density of whistler fluctuations, and γ_k is the instability growth rate obtained from Eq. (1). The unstable fluctuations scatter the electrons reducing their anisotropy. Dynamical equations describing temperature components $T_{a,\perp,\parallel}$ (the second order moments of the velocity distribution) are readily obtained from Eq. (2)

$$\frac{dT_{e,\perp}}{dt} = \frac{m_e}{2k_B} \frac{d}{dt} \int d^3v v_{\perp}^2 f_e \quad (4)$$

$$\frac{dT_{e,\parallel}}{dt} = \frac{m_e}{k_B} \frac{d}{dt} \int d^3v v_{\parallel}^2 f_e. \quad (5)$$

Detailed expressions of Eqs. (4) and (5) are given in Appendix C.

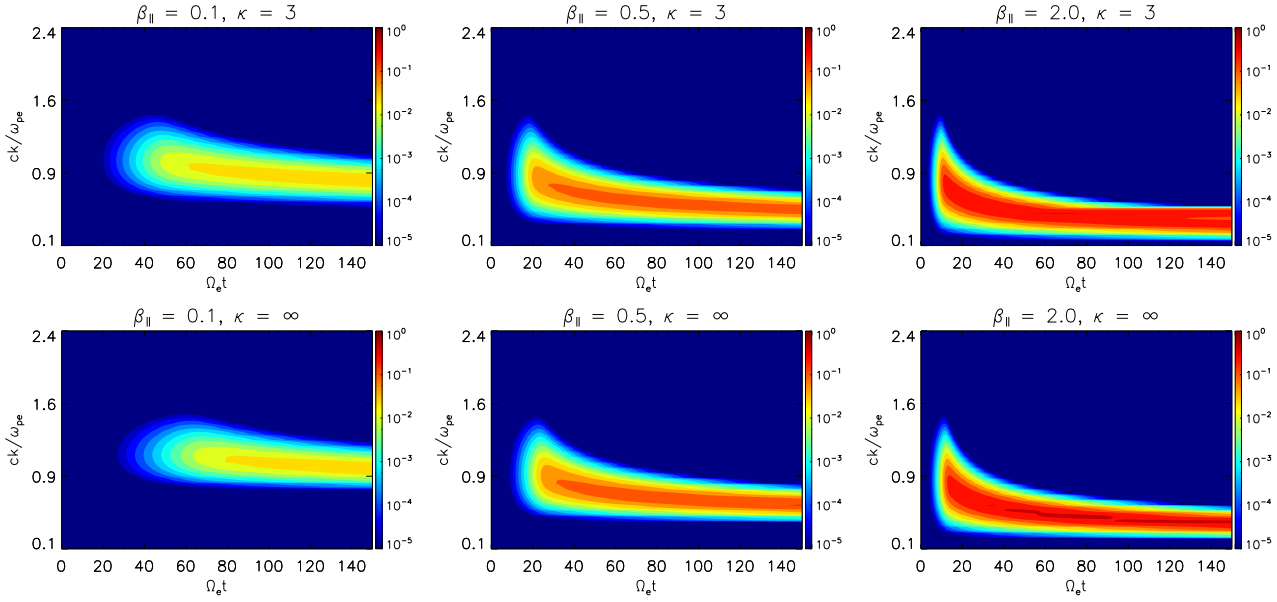


Fig. 2 Temporal evolution of the wave-number spectra of the color-coded (normalized) magnetic wave power, $\delta B^2(k)/B_0^2$, which is enhanced by the suprathermal electrons (upper panels) at early times.

In order to outline the effects of suprathermal electrons here we compare the unstable whistlers obtained for a bi-Kappa distribution, with the unstable solutions obtained only for the corresponding bi-Maxwellian core, which is usually considered when suprathermals are ignored. Fig. 1 illustrates linear and quasilinear solutions for three distinct cases corresponding to different (initial) plasma beta conditions $\beta_{c,\parallel}(0) = \beta_{\parallel}(0) = 0.1, 0.5, 2.0$, while the initial values of other parameters are the same, e.g., temperature anisotropy $A(0) = 4$ and power-index $\kappa = 3$. The first two rows on top display linear growth rates γ , which are all systematically enhanced by suprathermal electrons (red lines), and wave-frequencies ω_r showing only minor variations, with a decrease of the most unstable frequencies. The stimulative effect obtained for the growth rates is further confirmed in the quasilinear evolution of the instability by the magnetic wave-power $U_B = \int dk \delta B^2(k)/B_0^2$ of the whistler fluctuations, which shows the same systematic enhancement with an earlier initiation, a shorter growing time, and markedly higher saturation levels reached in the presence of suprathermals. The immediate consequence of the more intense fluctuations is a faster and more effective relaxation of the temperature anisotropy T_{\perp}/T_{\parallel} . All these effects of suprathermal electrons become more pronounced with increasing the plasma beta parameter, from left to right columns in Fig. 1. The highest levels of the fluctuating magnetic power are proportional with the increase of β_{\parallel} . For an initial $\beta_{\parallel}(0) = 2$ the anisotropy drops rapidly and de-

creases asymptotically to very low values approaching stable states of isotropic temperatures.

Fig. 2 displays temporal profiles of the full wave-number spectra of the magnetic power $\delta B^2(k)/B_0^2$, which show again an important increase in intensity in the presence of suprathermal electrons for all wave-numbers (upper panels). Magnetic power increases with increasing β_{\parallel} (from left to right), and an earlier ignition of the instability is also confirmed in this case.

An even more comprehensive and detailed picture is offered by the anisotropy thresholds plotted in Fig. 3, which describe the unstable solutions for a given value of the maximum growth rate γ_{\max} . Here we chose a low value $\gamma_{\max} = \gamma_m = 3 \times 10^{-3}|\Omega_e|$, approaching marginal stability and much lower than peaking values obtained in Fig. 1. The anisotropy thresholds predicted by the linear theory are fitted to

$$A_e = 1 + \frac{s}{\beta_{\parallel}^{\alpha}} \quad (6)$$

with $(s, \alpha) = (0.18, 0.52)$ for $\kappa = 3$ (red curve) and $(s, \alpha) = (0.29, 0.49)$ for $\kappa \rightarrow \infty$ (dashed black curve). All dynamical paths derived from QL theory for the same three cases in Fig. 1 converge to the same thresholds predicted by linear theory. The threshold values decrease under influence of suprathermal electrons (red curve), reconfirming their stimulative effect on whistler instability.

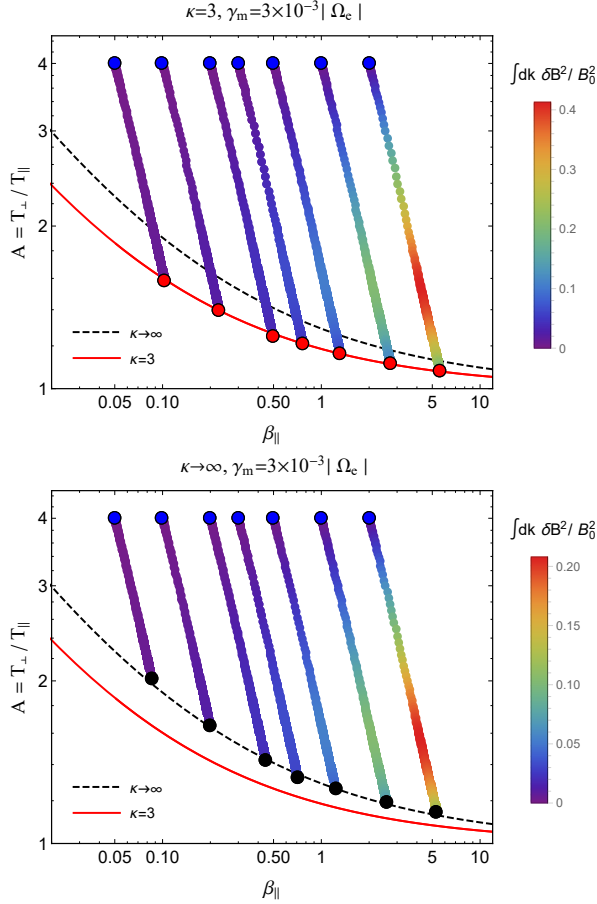


Fig. 3 QL dynamical paths end-up on the instability thresholds, which decrease in the presence of suprathermal electrons (red lines).

3 PIC simulations

For further examination in numerical experiments we have used one-dimensional particle-in-cell (PIC) simulations, and the results show a very good agreement with QL theory. Let us first describe the plasma parameters and the setup used in the simulations. We assume a collisionless and homogeneous plasma of electrons (subscript e) and protons (subscript p) in the same conditions considered in theory, i.e., with the same values for the plasma beta parameters, a realistic mass ratio $m_p/m_e = 1836$ and $\omega_{pe}/\Omega_e = 20$ for the plasma to cyclotron frequency ratio. Electrons are described by a bi-Kappa distribution function with the same initial $\beta_{\parallel} = 0.1, 0.05, 2$, corresponding to the three distinct cases considered in QL study, while protons are assumed Maxwellian and isotropic with $\beta_p = \beta_{\parallel}$. We used $n_x = 2048$ grid points and 10000 particles per grid cell, per species. The box size is $L_x = 512 c/\omega_{pe}$ in terms of the electron inertial length. The time step used is $\Delta t = 0.01/\omega_{pe}$ and the simulation runs until

$t_{\max} = 150/\Omega_e$. To construct the power spectra as functions of the wave-frequency ω or the wave-number k we have computed the Fourier-Laplace transforms of the magnetic field fluctuations in space and time.

Fig. 4 illustrates the time variation of the total magnetic power U_B (upper panels) and temperature anisotropy T_{\perp}/T_{\parallel} (bottom panels) obtained from PIC simulations for the three cases shown in Fig. 1. The qualitative and quantitative agreement with the results from QL theory is obvious, confirming that suprathermal electrons stimulate not only the instability growth rates and the resulting magnetic power, but implicitly also the relaxation of temperature anisotropy. In Fig. 5 we display the time evolution of the wave-number spectra of magnetic field fluctuations. The color scale corresponds to the magnetic field power, explicitly given by $|\text{FFT}_x(B_y - iB_z)|^2$, where FFT_x is the fast Fourier transform along the spatial dimension. These spectra agree very well with the corresponding ones from QL theory in Fig. 2. The saturation suggests a subsequent inverse cascade of the large-amplitude fluctuations towards lower wave-numbers, as already noticed by Kim et al. (2017) for Maxwellian plasmas.

Finally, in Fig. 6 we plot the total magnetic field power (integrated over the whole interval of time) in $\omega-k$ -space, enabling us to compare the trace of peaking intensities, with the dispersion relation $\omega_r(k)$ derived from linear theory, see also Hughes et al. (2016). These plots are showing only the magnetic field fluctuations, as $|\text{FFT}_{(x,t)}(B_y - iB_z)|^2$ in the color bar, where the fast Fourier transform is taken along the spatial and temporal dimensions. Though this comparison is not rigorously motivated, since the plasma conditions change in time, in Fig. 6 the pattern of peaking intensities resemble, especially for low-beta conditions ($\beta_{\parallel} = 0.1$), the linear dispersion (here shown with dashed lines) from Fig. 1. Notice again the enhancement of whistler fluctuations in the presence of suprathermals for all three cases (upper panels), which show the same increase of intensities with increasing plasmas beta (from left to right). Unfortunately, the quasithermal noise is enhanced in the same measure, and where present (shown is only the electromagnetic component), it may determine significant deviations from theoretical dispersion (dashed lines). Only solutions obtained for low-beta conditions, e.g., $\beta_{\parallel} = 0.1$ are less affected by the quasithermal noise and approach better the linear dispersion, as also shown in Hughes et al. (2016) for bi-Maxwellian electrons (see also their section V for more explanations on the effects of particle noise).

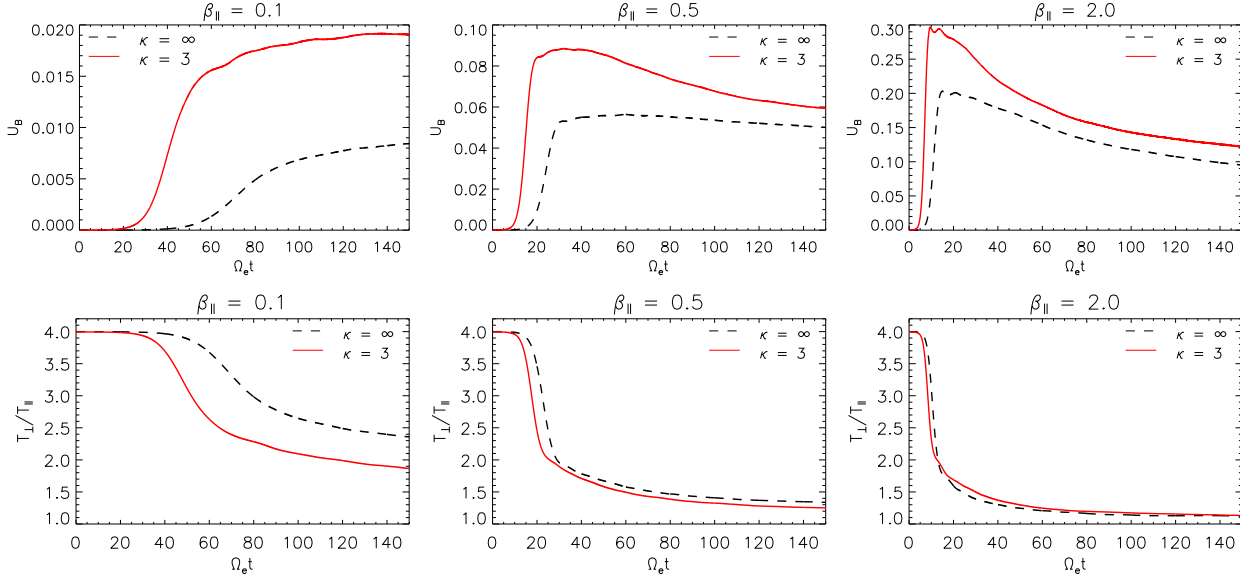


Fig. 4 Results from PIC simulations confirm a systematic stimulation of the magnetic power of whistler fluctuations (upper panels) and more efficient relaxation of temperature anisotropy in the presence of suprathermals, for the same three cases as in Fig. 1.

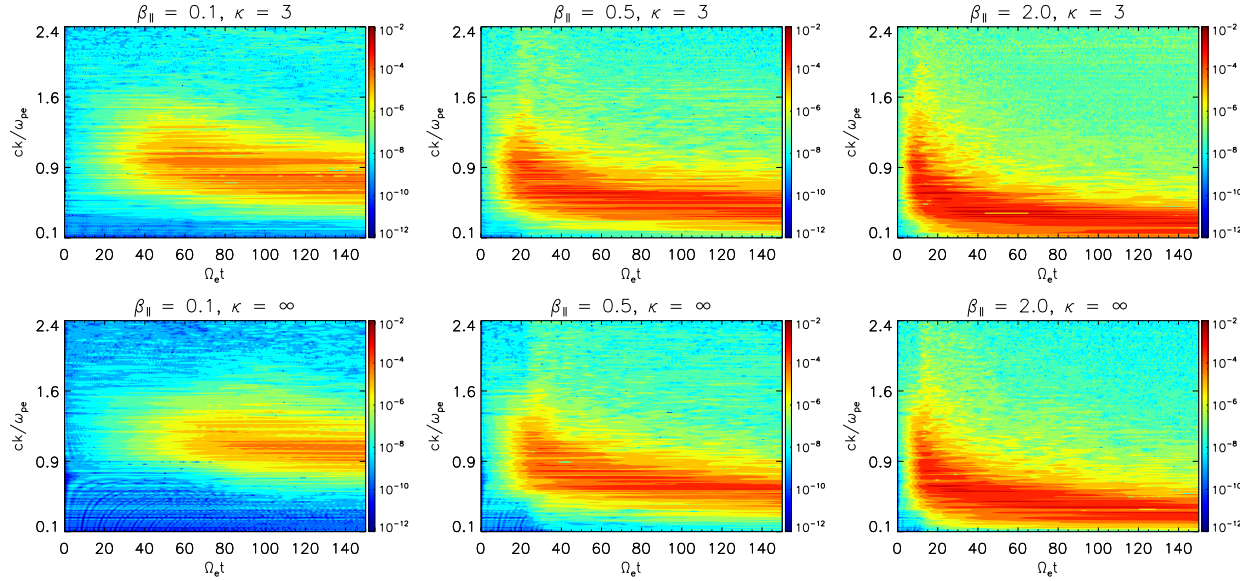


Fig. 5 Temporal evolutions for the wave-number spectra from PIC simulations confirming the enhancement effect of suprathermals (upper panels) predicted by the theory in Fig. 2. The color scale corresponds to the magnetic field power (see for details in the text).

4 Discussions and conclusions

Investigated here is the whistler instability driven by a temperature anisotropy $T_{\perp} > T_{\parallel}$ of electrons in conditions typically encountered in space plasmas, e.g., solar wind and planetary magnetospheres, where suprathermal particle populations are ubiquitous. Suprathermals enhance the high energy tails of the distributions, and overall, the observed velocity distributions are well

described by the Kappa power-laws, which are nearly Maxwellian at low energies and decrease as a power-law at higher energies. As motivated in section 1, we assume the anisotropic electrons well described by a single bi-Kappa distribution function. Deviations from thermal equilibrium suggest an additional source of free energy in the presence of suprathermal electrons, that may be released through the effect of instabilities, as

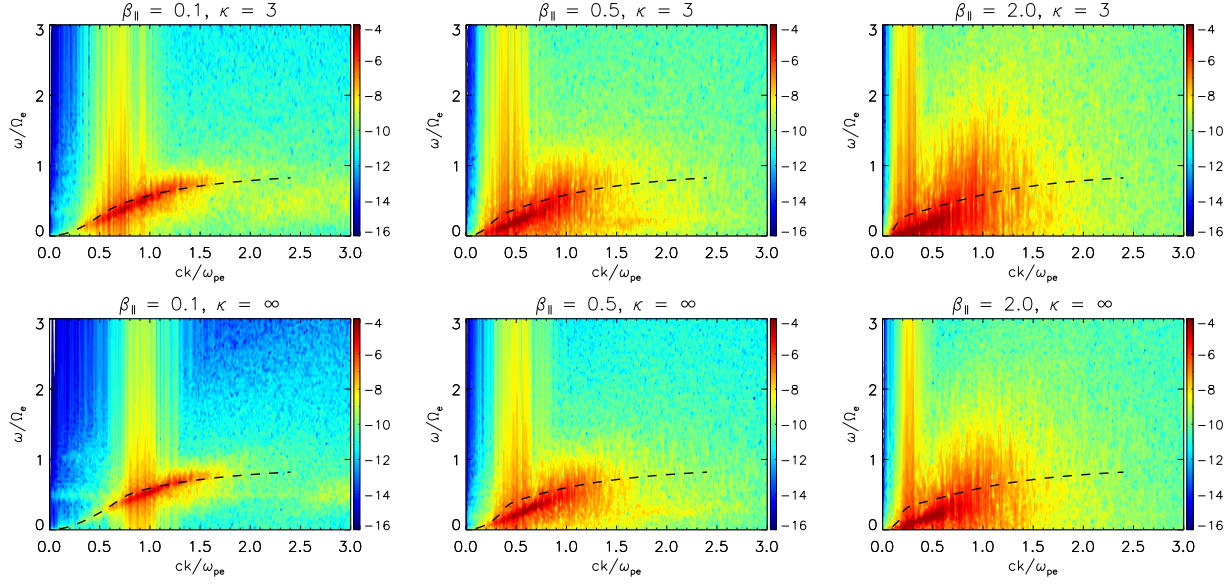


Fig. 6 Whistler fluctuations from PIC simulations resemble linear dispersion in the $(\omega - k)$ -space and are enhanced in the presence of suprathermals (lower panels), and with increasing β_{\parallel} (from left to right). The color scale corresponds to the magnetic field power (see for details in the text).

already suggested by linear theory (Lazar et al. 2015, 2017b). In order to capture these mutual effects, here we have used a quasilinear (QL) kinetic approach and PIC simulations, which allowed us to characterize the long-term evolution of the instability under the influence of suprathermal electrons.

To outline the effects of suprathermal electrons we have invoked a straightforward comparison of the observed bi-Kappa distribution with the quasi-thermal bi-Maxwellian core, which is solely considered when suprathermal (halo) populations are ignored. The same method has already been applied in linear theory that confirms the expectations showing an enhancement of the instability growth-rates in the presence of suprathermal electrons. (and not only for whistler instability, as already shown in the Introduction). For whistlers enhanced growth-rates are plotted in Fig. 1, top line panels, for three distinct cases corresponding to $\beta_{\parallel} = 0.1, 0.5, 2$. We have chosen these cases as representative for a large variety of space plasma conditions, ranging from low-beta plasmas in the outer corona or terrestrial magnetosphere, to a high-beta solar wind at large heliospheric distances. In addition, the results obtained here from QL theory and simulations are in perfect agreement, and show a systematic stimulation (no inhibition) of the spectral and total magnetic power of whistler fluctuations. Moreover, a direct consequence of larger amplitude fluctuations is their back effect on the anisotropic distributions, which show a faster and more efficient relaxation in the presence of suprathermals. We have also shown that these effects markedly

increase with increasing the plasma beta parameter. These results support the hypothesis that suprathermal populations are an important source of free energy, which stimulate the kinetic instabilities and implicitly, the relaxation of the non-equilibrium collisionless plasmas from space. Moreover, our present results should also stimulate future studies on instabilities of different nature, like firehose instabilities driven by an opposite anisotropy of temperature $T_{\parallel} > T_{\perp}$, or beam-plasma instabilities with an influence of drifting suprathermals like the so-called electron strahl very often reported by the observations in the solar wind.

Acknowledgements The authors acknowledge support from the Katholieke Universiteit Leuven and Ruhr-University Bochum. These results were obtained in the framework of the projects SCHL 201/35-1 (DFG-German Research Foundation), GOA/2015-014 (KU Leuven), G0A2316N (FWO-Vlaanderen), and C 90347 (ESA Prodex 9). S.M. Shaaban would like to acknowledge the support by a Postdoctoral Fellowship (Grant No. 12Z6218N) of the Research Foundation Flanders (FWO-Belgium).

Appendix A: Kappa vs. Maxwellian models

In the presence of a suprathermal population the electrons are described by a bi-Kappa velocity distribution

function (Summers and Thorne 1991)

$$f_\kappa(v_{\parallel}, v_{\perp}) = \frac{1}{\pi^{3/2} u_{\perp}^2 u_{\parallel}} \frac{\Gamma(\kappa + 1)}{\kappa^{3/2} \Gamma(\kappa - 1/2)} \times \left[1 + \frac{v_{\parallel}^2}{\kappa u_{\parallel}^2} + \frac{v_{\perp}^2}{\kappa u_{\perp}^2} \right]^{-\kappa-1} \quad (7)$$

which is normalized to unity $\int d^3v f_\kappa = 1$ and is written in terms of normalization velocities $u_{\parallel, \perp}$ related to the components of kinetic temperature (for $\kappa_e > 3/2$)

$$T_{\kappa, \parallel} = \frac{m}{k_B} \int d^3v v_{\parallel}^2 f_\kappa(v_{\parallel}, v_{\perp}) = \frac{\kappa}{\kappa - 3/2} \frac{m_e u_{\parallel}^2}{2k_B},$$

$$T_{\kappa, \perp} = \frac{m}{2k_B} \int d^3v v_{\perp}^2 f_\kappa(v_{\parallel}, v_{\perp}) = \frac{\kappa}{\kappa - 3/2} \frac{m_e u_{\perp}^2}{2k_B}. \quad (8)$$

Suprathermals enhance the high energy tails of the observed distributions, highly contrasting with the quasi-thermal core (subscript c) which is well described by a standard bi-Maxwellian model (Lazar et al. 2015, 2016)

$$f_c(v_{\parallel}, v_{\perp}) = \frac{1}{\pi^{3/2} u_{\perp}^2 u_{\parallel}} \exp \left(-\frac{v_{\parallel}^2}{u_{\parallel}^2} - \frac{v_{\perp}^2}{u_{\perp}^2} \right), \quad (9)$$

where $u_{\parallel, \perp}$ become thermal velocities corresponding to the temperature components

$$T_{c, \parallel} = \frac{m}{k_B} \int d^3v v_{\parallel}^2 f_c(v_{\parallel}, v_{\perp}) = \frac{m u_{c, \parallel}^2}{2k_B},$$

$$T_{c, \perp} = \frac{m}{2k_B} \int d^3v v_{\perp}^2 f_c(v_{\parallel}, v_{\perp}) = \frac{m u_{c, \perp}^2}{2k_B}. \quad (10)$$

By comparison to the Maxwellian core, suprathermals also enhance the electron kinetic (energy) temperature (Lazar et al. 2015)

$$T_{\kappa, \parallel, \perp} = \frac{\kappa}{\kappa - 3/2} T_{c, \parallel, \perp} > T_{c, \parallel, \perp}, \quad (11)$$

and implicitly the plasma beta parameter

$$\beta_{\kappa, \parallel, \perp} = \frac{\kappa_e}{\kappa_e - 3/2} \beta_{c, \parallel, \perp} > \beta_{c, \parallel, \perp} \equiv \beta_{\parallel, \perp}. \quad (12)$$

The anisotropy does not depend on κ and we can write generically

$$A \equiv \frac{T_{\perp}}{T_{\parallel}} = \frac{T_{\kappa, \perp}}{T_{\kappa, \parallel}} = \frac{T_{c, \perp}}{T_{c, \parallel}}. \quad (13)$$

Playing only the role of a neutralizing background, the much heavier protons do not react to high-frequency modes, and, for simplicity, we can consider them isotropic and Maxwellian distributed with $\beta_p = \beta_{\parallel}$.

Appendix B: Plasma dispersion functions

For the dispersion theory of Kappa distributed plasma we use the modified Kappa dispersion function (Lazar et al. 2008)

$$Z_\kappa(\xi_\kappa^\pm) = \frac{1}{\pi^{1/2} \kappa^{1/2}} \frac{\Gamma(\kappa)}{\Gamma(\kappa - 1/2)} \times \int_{-\infty}^{\infty} \frac{(1 + x^2/\kappa)^{-\kappa}}{x - \xi_\kappa^\pm} dx, \quad \Im(\xi_\kappa^\pm) > 0. \quad (14)$$

In the Maxwellian limit $\kappa \rightarrow \infty$ the plasma dispersion function takes the following standard form (Fried and Conte 1961)

$$Z(\xi^\pm) = \frac{1}{\pi^{1/2}} \int_{-\infty}^{\infty} \frac{\exp(-x^2)}{x - \xi^\pm} dt, \quad \Im(\xi^\pm) > 0, \quad (15)$$

which is used to describe the dispersion and stability of the electron core population, when suprathermals are neglected. The proton term (subscript p) in Eq. (1) contains the same plasma dispersion function Z .

Appendix C: Dynamical equations for the temperature components

Time evolutions of the second order moments giving the components of electron temperature are obtained using (2) in Eqs. (4) and (5) (Shaaban et al. 2019b)

$$\frac{dT_{\perp}}{dt} = -\frac{e^2}{2m_e k_B c^2} \int_{-\infty}^{\infty} \frac{dk}{k^2} \langle \delta B^2(k) \rangle \times \left((2A - 1) \gamma + \text{Im} \left[\frac{2i\gamma + \Omega_e}{ku_{\parallel}} G \right] \right), \quad (16)$$

$$\frac{dT_{\parallel}}{dt} = \frac{e^2}{m_e k_B c^2} \int_{-\infty}^{\infty} \frac{dk}{k^2} \langle \delta B^2(k) \rangle \times \left(A \gamma + \text{Im} \left[\frac{\omega + \Omega_e}{ku_{\parallel}} G \right] \right), \quad (17)$$

with

$$G = [A \omega \pm \Omega_e (A - 1)] Z_\alpha \left(\frac{\omega - |\Omega_e|}{ku_{\parallel}} \right), \quad (18)$$

where $Z_\alpha = Z$ for the Maxwellian core and $Z_\alpha = Z_\kappa$ for the observed Kappa distribution function.

References

- An, X., Yue, C., Bortnik, J., Decyk, V., Li, W., Thorne, R.M.: *Journal of Geophysical Research (Space Physics)* **122**(2), 2001 (2017)
- Fried, B., Conte, S.: *The Plasma Dispersion Function*. New York: Academic Press, ??? (1961). doi:10.1016/B978-1-4832-2929-4.50005-8
- Gary, S.: *Theory of Space Plasma Microinstabilities*, Cambridge Univ, (1993)
- Hapgood, M., Perry, C., Davies, J., Denton, M.: *Planet. Space Sci.* **59**(7), 618 (2011)
- Hughes, R.S., Wang, J., Decyk, V.K., Gary, S.P.: *Physics of Plasmas* **23**(4), 042106 (2016)
- Kellogg, P.J., Cattell, C.A., Goetz, K., Monson, S.J., Wilson, I. L. B.: *Journal of Geophysical Research (Space Physics)* **116**(A9), 09224 (2011)
- Kennel, C.F., Petschek, H.E.: *Journal of Geophysical Research* **71**(1), 1 (1966)
- Kim, H.P., Hwang, J., Seough, J.J., Yoon, P.H.: *Journal of Geophysical Research (Space Physics)* **122**(4), 4410 (2017)
- Lazar, M., Fichtner, H., Yoon, P.H.: *Astron. Astrophys.* **589**, 39 (2016)
- Lazar, M., Poedts, S., Fichtner, H.: *Astron. Astrophys.* **582**, 124 (2015)
- Lazar, M., Poedts, S., Michno, M.J.: *Astron. Astrophys.* **554**, 64 (2013)
- Lazar, M., Schlickeiser, R., Shukla, P.K.: *Physics of Plasmas (1994-present)* **15**(4), 042103 (2008)
- Lazar, M., Poedts, S., Schlickeiser, R., Dumitache, C.: *Mon. Not. R. Astron. Soc.* **446**, 3022 (2015)
- Lazar, M., Pierrard, V., Shaaban, S.M., Fichtner, H., Poedts, S.: *Astron. Astrophys.* **602**, 44 (2017a)
- Lazar, M., Shaaban, S.M., Poedts, S., Štverák, Š.: *Mon. Not. R. Astron. Soc.* **464**(1), 564 (2017b)
- Lazar, M., Yoon, P.H., López, R.A., Moya, P.S.: *Journal of Geophysical Research (Space Physics)* **123**(1), 6 (2018a)
- Lazar, M., Kim, S., López, R.A., Yoon, P.H., Schlickeiser, R., Poedts, S.: *Astrophys. J.* **868**(2), 25 (2018b). doi:10.3847/2041-8213/aaefec
- Mace, R.L., Sydora, R.D.: *Journal of Geophysical Research (Space Physics)* **115**(A7), 07206 (2010)
- Maksimovic, M., Zouganelis, I., Chaufray, J.-Y., Issautier, K., Scime, E., Littleton, J., Marsch, E., McComas, D., Salem, C., Lin, R., et al.: *Journal of Geophysical Research: Space Physics* **110**(A9) (2005)
- Maksimovic, M., Pierrard, V., Riley, P.: *Geophysical research letters* **24**(9), 1151 (1997)
- Pierrard, V., Lazar, M.: *Solar Physics* **267**(1), 153 (2010)
- Pierrard, V., Lazar, M., Poedts, S., Štverák, Š., Maksimovic, M., Trávníček, P.M.: *Solar Physics* **291**(7), 2165 (2016). doi:10.1007/s11207-016-0961-7
- Schriger, D., Ashour-Abdalla, M., Coroniti, F.V., LeBoeuf, J.N., Decyk, V., Travnicek, P., Santolík, O., Winningham, D., Pickett, J.S., Goldstein, M.L.: *Journal of Geophysical Research (Space Physics)* **115**(9), 00 (2010)
- Shaaban, S.M., Lazar, M., Poedts, S., Elhanbaly, A.: *Astrophys. Space Sci.* **361**(6), 193 (2016)
- Shaaban, S.M., Lazar, M., Poedts, S., Elhanbaly, A.: *Astrophys. Space Sci.* **362**(1), 13 (2017)
- Shaaban, S.M., Lazar, M., Astfalk, P., Poedts, S.: *Journal of Geophysical Research (Space Physics)* **123**(3), 1754 (2018)
- Shaaban, S.M., Lazar, M., López, R.A., Fichtner, H., Poedts, S.: *Mon. Not. R. Astron. Soc.* **483**(4), 5642 (2019a)
- Shaaban, S.M., Lazar, M., Yoon, P.H., Poedts, S.: *Astrophys. J.* **871**(2), 237 (2019b)
- Stenzel, R.L.: *J. Geophys. Res.* **104**(A7), 14379 (1999)
- Štverák, Š., Trávníček, P., Maksimovic, M., Marsch, E., Fazakerley, A.N., Scime, E.E.: *Journal of Geophysical Research: Space Physics* **113**(A3) (2008)
- Summers, D., Thorne, R.M.: *Physics of Fluids B: Plasma Physics* (1989-1993) **3**(8), 1835 (1991)
- Vasyliunas, V.M.: *Journal of Geophysical Research* **73**(9), 2839 (1968)
- Viñas, A.F., Moya, P.S., Navarro, R.E., Valdivia, J.A., Araneda, J.A., Muñoz, V.: *Journal of Geophysical Research: Space Physics* **120**(5), 3307 (2015)
- Wilson III, L.B., Cattell, C.A., Kellogg, P.J., Goetz, K., Kersten, K., Kasper, J.C., Szabo, A., Meziane, K.: *Journal of Geophysical Research (Space Physics)* **114**(A10), 10106 (2009)
- Wilson III, L.B., Koval, A., Szabo, A., Breneman, A., Cattell, C.A., Goetz, K., Kellogg, P.J., Kersten, K., Kasper, J.C., Maruca, B.A., Pulupa, M.: *Journal of Geophysical Research: Space Physics* **118**(1), 5 (2013). doi:10.1029/2012JA018167
- Wilson III, L.B., Chen, L.-J., Wang, S., Schwartz, S.J., Turner, D.L., Stevens, M.L., Kasper, J.C., Osmane, A., Caprioli, D., Bale, S.D., Pulupa, M.P., Salem, C.S., Goodrich, K.A.: *The Astrophysical Journal Supplement Series* **243**(1), 8 (2019). doi:10.3847/1538-4365/ab22bd
- Yoon, P.H.: *Reviews of Modern Plasma Physics* **1**, 4 (2017)